reexamination after the FOB test, placing excessive physical and physiologic burdens on examiners and examinees, as well as imposing an undue financial burden upon society. The only approved screening alternative to FOB for the diagnosis of colorectal cancer is testing for the tumor marker carcinoembryonic antigen (CEA). Unfortunately, CEA is not useful as a marker for the early detection of colorectal cancer (11). Therefore, it is necessary to identify a new biomarker to supplement these current diagnostic modalities.

Alterations in the protein content of clinical samples reflect the dynamic biological changes of patients more directly than changes in mRNA levels (12). Plasma/serum proteins are thus valuable resources for the discovery of biomarkers with direct clinical application. We previously developed a quantitative proteomics platform called 2-dimensional image converted analysis of liquid chromatography and mass spectrometry (2DICAL; ref. 13). This technology is especially advantageous in clinical studies in which a large number of patient samples must be compared. We were able to identify a number of plasma/serum biomarkers with high potential for clinical application using 2DICAL (14–18). However, the direct analysis of plasma/serum proteins using 2DICAL remains technically challenging. Proteins secreted by cancer cells are considerably diluted in the blood circulation and present only in a low concentration (19, 20). The concentration of serum/plasma proteins ranges over more than 10 orders of magnitude and thus the efficient removal of abundant plasma/serum proteins is essential for the detection of low-abundance cancer-related biomarker proteins (21).

In this study, we applied a high-performance hollow-fiber membrane (HFM) technology to the enrichment of low-molecular weight (LMW) proteins (17, 22) and searched for new plasma biomarkers that might be applicable to the early diagnosis of colorectal cancer. The LMW plasma protein fraction is made up of various functional proteins, such as cytokines, chemokines, and peptides and is considered to be a rich unexplored archive of biological information (20). The HFM-based technique (HFMT) utilizes a fully automated system that can separate and concentrate low-abundance plasma proteins from relatively high-molecular weight abundant proteins such as albumin, immunoglobulin, transferrin, and apolipoproteins with high efficiency and reproducibility (22). Here, we report the identification of adipophilin, an adipose differentiation–related protein, as a novel tumor marker for colorectal cancer through a comprehensive analysis of the LWM plasma proteome of colorectal cancer patients using HFM and 2DICAL technologies.

Patients and Methods

Plasma samples

Plasma samples were collected prospectively from 366 individuals and then split randomly into 3 cohorts [training, validation-1 (V1), and validation-2 (V2); Table 1]. The cohorts were essentially hospital based and consisted of healthy volunteers and newcomers (primarily to gastrointestinal services) between August 2006 and October 2008 at the following 7 hospitals in Japan: National Cancer Center Hospital (NCCH; Tokyo), Osaka National Hospital (ONH; Osaka), Jichi Medical School Hospital (JMS; Shimotsuke), Osaka Medical Center for Cancer and Cardiovascular Diseases (Osaka), Tokyo Medical University Hospital (TMUH; Tokyo), Osaka Medical College Hospital (OMC; Osaka), and Fukuoka University Hospital (Fukuoka). This multi-institutional collaborative study group was organized by the "Third-Term Comprehensive Control Research for Cancer" conducted by the Ministry of Health, Labour and Welfare of Japan and joined the International Cancer Biomarker Consortium (23). Written informed consent was obtained from every subject.

All patients diagnosed as having cancer had histologic or cytologic proof of colorectal adenocarcinoma. Demographic and laboratory data for the cases are summarized in Table 1. The staging of cancer was defined according to TNM classification by the International Union against Cancer (UICC). The Training cohort comprised 43 cases, including untreated colorectal cancer patients from TMUH ($n = 8$), JMS ($n = 9$), and ONH ($n = 5$), and healthy controls from NCCH ($n = 2$), TMUH ($n = 9$), OMC ($n = 6$), and ONH ($n = 4$). The V1 and V2 cohorts comprised 210 and 113 cases, respectively, from the 7 hospitals as described above. The V1 cohort included 101 patients with colorectal cancer and 109 healthy controls. The V2 cohort comprised 26 patients with colorectal cancer and 87 healthy controls.

For all the samples used in this study, the same protocol was used for blood collection, storage, and freeze/thawing to ensure absence of any preanalytical bias caused by differences in sample handling. Blood was collected in a tube with EDTA at the time of diagnosis. Plasma was separated by centrifugation and frozen at −80°C until analysis. Macroscopically hemolyzed samples were excluded from the present analysis. The protocol of this study was reviewed and approved by the institutional ethics committee board of each participating institute.

Depletion of high-molecular weight plasma proteins

The plasma samples of the training cohort were filtered through a 0.22-μm pore size filter. Five hundred microliter of the sample was diluted by adding 3.5 mL 25 mmol/L ammonium bicarbonate buffer (pH 8.0). The total of 4 mL of the plasma dilution was injected into a HFMT machine (22). After 1 hour of fully automated operation, the solution containing LMW proteins was recovered and lyophilized.

Liquid chromatography mass spectrometry

The HFMT-treated samples were digested with sequencing grade modified trypsin (Promega) and analyzed in duplicate using a nano flow high-performance

Table 1. Clinicopathologic characteristics of cases in the training ($n = 43$) and validation cohorts (V1: $n = 210$; V2: $n = 113$)

	Training cohort ($n = 43$)			Validation-1 cohort ($n = 210$)			Validation-2 cohort ($n = 113$)		
	Cancer	Healthy	*P*	Cancer	Healthy	*P*	Cancer	Healthy	*P*
No. of patients	22	21		101	109		26	87	
Sex, no. of patients			0.310[a]			0.782[a]			0.252[a]
Male	14	17		63	70		13	56	
Female	8	4		38	39		13	31	
Age, y			<0.001			<0.001			<0.001
Mean (SD)	62 (12)	40 (13)		64 (11)	42 (14)		63 (12)	43 (16)	
Tumor location			*NA*			*NA*			*NA*
Colon	22	Ð		88	Ð		24	Ð	
Rectum	0	Ð		13	Ð		2	Ð	
Clinical stage			*NA*			*NA*			*NA*
I	3	Ð		19	Ð		12	Ð	
II	6	Ð		31	Ð		5	Ð	
III	8	Ð		32	Ð		8	Ð	
IV	5	Ð		17	Ð		1	Ð	
Unknown	0	Ð		2	Ð		0	Ð	
CA19-9									
Median, U/mL	14.7	5.5	0.010	4	1.6	<0.001	9.4	10.2	0.680
>37.0 (ULN), no. of patients	6	2		39	5		2	4	
CEA									
Median, ng/mL	3.5	1.7	0.002	11.8	7.6	0.001	2.6	1.7	0.008
>5.0 (ULN), no. of patients	9	1		24	5		4	5	
Total bilirubin									
Median, mg/dL	0.4	0.5	0.114	0.4	0.5	<0.001	0.4	0.5	<0.001
>1.2 (ULN), no. of patients	0	0		1	3		0	4	
Adipophilin									
Mass spectrometry peak intensity[b], mean (SD)	320 (375)	96 (78)	<0.001[c]	Ð	Ð		Ð	Ð	
Protein intensity[d], mean (SD)	Ð	Ð		3.91 (0.06)	3.82 (0.13)	<0.001[e]	3.57 (0.14)	3.42 (0.20)	<0.001[e]

NOTE: Wilcoxon test was applied to assess differences between values.

Abbreviations: NA, not applicable; ULN, upper limit of normal.

[a]Calculated by Fisher's exact test.

[b]Intensity of the corresponding peak as measured using quantitative mass spectrometry.

[c]Calculated using Mann–Whitney *U* test.

[d]Measured using reverse-phase protein microarray (logarithmic variable).

[e]Calculated using Welch's *t*-test.

liquid chromatography (NanoFrontier nLC; Hitachi High-technologies) connected to an electrospray ionization quadrupole time-of-flight (ESI-Q-TOF) mass spectrometer (Q-Tof Ultima; Waters).

Mass spectrometry (MS) peaks were detected, normalized, and quantified using the in-house 2DICAL software package, as described previously (13). A serial identification (ID) number was applied to each of the MS peaks detected (1 to 53,009). The stability of liquid chromatography mass spectrometry (LC-MS) was monitored by calculating the correlation coefficient (CC) and coefficient of variance (CV) of every measurement. For all 53,009 peaks observed in the 43 duplicate runs, the mean CC (± SD) was as high as 0.951 (± 0.039) and the mean CV was as low as 0.054 (± 0.011).

Protein identification by tandem mass spectrometry

Peak lists were generated using the Mass Navigator software package (version 1.2; Mitsui Knowledge Industry) and the peak lists were searched against the SwissProt database (downloaded on April 22, 2009) using the Mascot software package (version 2.2.1; Matrix Science). The search parameters used were as follows: the human protein database was selected; up to 1 missed cleavage was allowed; "none" was designated as the enzyme; mass tolerances for precursor and fragment ions were ± 0.6 and

± 0.2 Da, respectively; the score threshold was set to $P < 0.05$ on the basis of size of the database used in the search. If a peptide matched multiple proteins, the protein name with the highest Mascot score was selected.

Immunoblot analysis

Primary antibodies used were mouse monoclonal antibody (mAb) against adipophilin (LifeSpan Biosciences) and mouse mAb against human complement C3b-α (Progen). Ten microliter of 1:50 diluted plasma sample and 0.3 μg of fully recombinant adipophilin (BioVendor) as positive control were separated by SDS-PAGE and electroblotted onto a polyvinylidene difluoride membrane. The membrane was then incubated with primary antibody followed by horseradish peroxidase (HRP)-conjugated anti-mouse IgG as described previously (24, 25). Blots were developed using an enhanced chemiluminescence detection system (GE Healthcare).

Reverse-phase protein microarray

The plasma samples from the V1 and V2 cohorts were serially diluted 1:32, 1:64, 1:128, and 1:256 using a Biomek 2000 Laboratory Automation Robot (Beckman Coulter), and randomly plotted onto ProteoChip glass slides (Proteogen) in quadruplicate in a 6144-spot/slide format using a Protein Microarrayer Robot (Kaken Geneqs). The spotted slides were incubated overnight with the same primary antibody as used in Western blotting. The slides were incubated with biotinylated anti-mouse IgG (Vector Laboratories) followed by streptavidin–HRP conjugate (GE Healthcare). Peroxidase activity was detected using the Tyramide Signal Amplification Cyanine 5 System (PerkinElmer). The slides were counterstained with Alexa Fluor 546–labeled goat anti-human IgG (Invitrogen; spotting control).

The stained slides were scanned on a microarray scanner (InnoScan 700AL; Innopsys). Fluorescence intensity, determined as mean values of quadruplicate samples, was determined using the Mapix software (Innopsys). All intensity values were transformed into logarithmic variables. The reproducibility of our reverse-phase protein microarray assay was reported previously (18).

Immunohistochemistry

Twenty colorectal cancer cases were selected from the surgical pathology archive panel of the National Cancer Center Hospital, as described previously (24). Sections (4-μm thick) were cut from paraffin blocks of colorectal cancer tissues and mounted on silanized glass slides and were subsequently stained by the avidin–biotin complex method. The primary antibody was the same as used in immunoblot analysis.

Statistical analysis

The statistical significance of intergroup differences was assessed with the Wilcoxon test, Mann–Whitney *U* test, Welch's *t* test, Kruskal–Wallis test, or Fisher's exact test, as appropriate. The area under the curve (AUC) value of the receiver operating characteristics (ROC) analysis was calculated for each marker to evaluate its diagnostic significance using ROCKIT software (version 0.9.1; the Kurt Rossmann Laboratories). A composite index of 2 markers was generated using the result of multivariate logistic regression analysis, which also enabled the calculation of sensitivity, specificity, and ROC curves. Statistical analyses were done using an open-source statistical language R (version 2.7.0) with the optional module Design package.

Results

Plasma biomarker discovery by quantitative MS

To identify a diagnostic biomarker for patients with colorectal cancer including those with early-stage diseases, we compared the plasma proteomes of 22 colorectal cancer patients with those of 21 healthy controls (training cohort) using 2DICAL (Table 1). Among a total of 53,009 independent MS peaks detected within the range 250 to 1,600 *m/z* and within the time range 20 to 70 minutes, we found 103 peaks with a discriminatory AUC value of >0.800. A representative 2-dimensional view of all the MS peaks, with the *m/z* displayed along the X-axis and the LC retention time (RT) along the Y-axis, is shown in Figure 1A. The 103 MS peaks which distinguished between colorectal cancer patients and healthy controls with AUC values of >0.800 are highlighted in red.

Eleven tandem mass spectrometry spectra acquired from those 103 peaks matched 6 proteins in the database with Mascot score >40 (Supplementary Table S1). We focused attention on a MS peak (ID 83) derived from the amino acid sequence of *ADFP* gene product (Supplementary Fig. S1) because the expression level of adipophilin was previously reported to be upregulated in clear cell renal carcinoma, but no such upregulation has been described in colorectal cancer. The adipophilin-derived MS peak (ID 83, at 749 *m/z* and 47.4 minutes) in representative patients from cancer and control groups is shown in Figure 1B. The distribution of the MS peak (ID 83) in patients with colorectal cancer (red) and healthy controls (blue) in the training cohort (AUC = 0.814) is shown in Figure 1C. The differential expression and identification of adipophilin was confirmed by denaturing SDS-PAGE and immunoblotting analyses (Fig. 1D).

Protein microarray validation

To further validate the utility of using adipophilin for the diagnosis of colorectal cancer, the relative level of adipophilin in a total of 323 plasma samples was quantified using reverse-phase protein microarrays (Fig. 2). Quadruplicate spots for representative cases with high and low levels of adipophilin are shown in Figure 2. The power of plasma adipophilin level to discriminate colorectal cancer was validated in 2 larger independent validation cohorts (V1: $n = 210$, V2: $n = 113$) that included early-stage colorectal cancer (Table 1). In the V1 cohort, the adipophilin level was significantly higher in patients

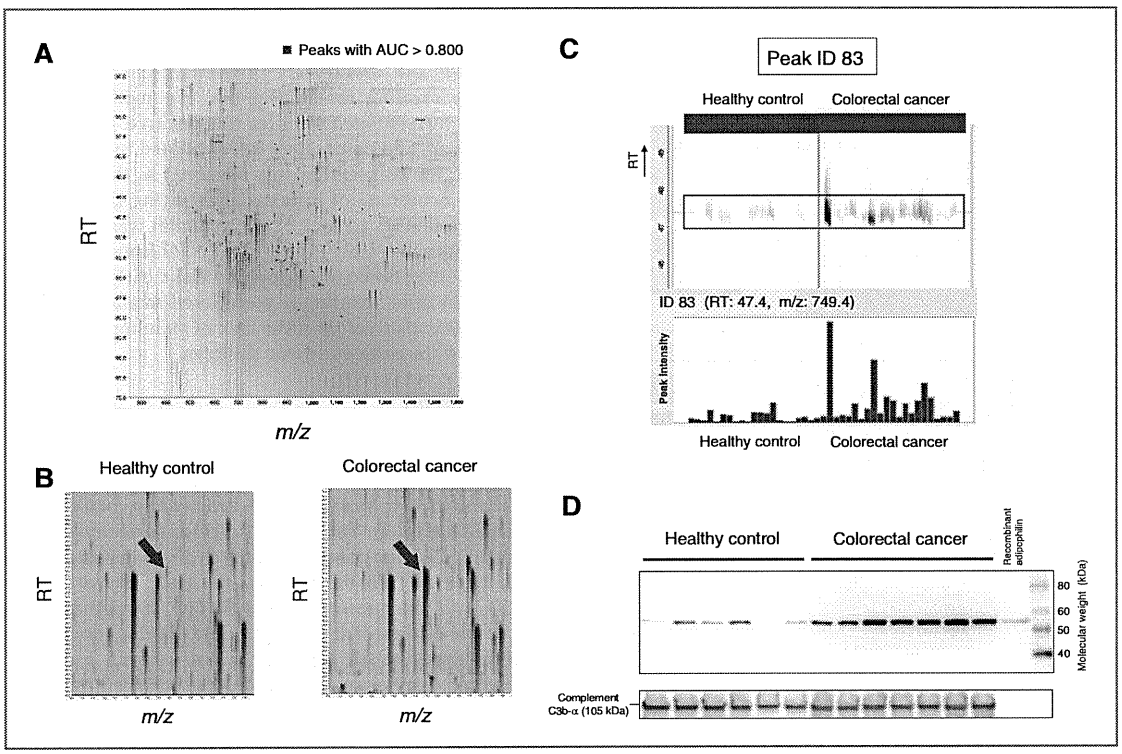

Figure 1. A, two-dimensional display of all (>53,000) MS peaks detected. The 103 MS peaks for which the mean intensity determined in duplicate analyses distinguished between colorectal cancer and healthy control patients (with AUC values >0.800) are highlighted in red. B, adipophilin-derived MS peaks in representative patients from cancer and control groups. Arrows indicate ID 83, at 749 *m/z* and a RT of 47.4 minutes. C, adipophilin-derived MS peaks (ID 83) in 43 duplicate LC-MS runs aligned according to RT (top). Columns represent the mean intensity of duplicate analyses of the 43 individuals in the training cohort (bottom). D, verification of quantitative MS data and protein identification. The levels of plasma adipophilin and complement C3b-α (loading control) were determined using immunoblotting in representative colorectal cancer patients and healthy individuals selected from the training cohort. Recombinant adipophilin (0.3 μg) was applied as a positive control (lane next to the molecular weight standard ladder).

with colorectal cancer than in healthy controls (Welch's t test $P = 5.49 \times 10^{-10}$, Fig. 3A and Table 1), with an AUC value of 0.767 (95% CI: 0.699–0.825; Fig. 3B). The colorectal cancer discriminatory power of adipophilin was also apparent in the V2 cohort ($P = 0.00009$, Fig. 3C and Table 1), with an AUC value of 0.742 (95% CI: 0.625–0.836; Fig. 3B).

There was no difference in the plasma level of adipophilin among different disease stages (Kruskal–Wallis test $P = 0.280$). Notably, however, the adipophilin level was significantly higher even in patients with stage I or II disease (localized early colorectal cancer without metastasis to lymph nodes) than in healthy controls, whereas the CEA level in early-stage patients did not significantly differ from that of healthy controls (Table 2).

Adipophilin complements CEA

The levels of adipophilin and CEA were not mutually correlated (Pearson's $r = 0.13$ in the V1 cohort and 0.12 in the V2 cohort), and the AUC values of CEA in both cohorts (Fig. 3D) were comparable with that of a previous report (26). Combining adipophilin and CEA quantitation yielded a significant improvement in the ability to distinguish patients with colorectal cancer from healthy controls compared with quantitating CEA alone; the AUC improved to 0.849 (95% CI: 0.790–0.896) in the V1 cohort ($P = 0.0008$) and 0.787 (0.673–0.874) in the V2 cohort ($P = 0.022$; Fig. 3D), indicating that plasma adipophilin and CEA have complementary diagnostic utility.

Due to the low prevalence of colorectal cancer among an asymptomatic population, a high specificity is required for a screening biomarker. If we defined the upper limit of the normal range of the composite index (adipophilin plus CEA; Fig. 3D) to include 95% of healthy controls in each validation cohort, the sensitivity of the index was 54% (95% CI: 41–66) in the V1 cohort and 31% (13–56) in the V2 cohort.

Adipophilin expression in colorectal cancer

The expression and cellular distribution of adipophilin in colorectal cancer tissues were examined using an immunohistochemical assay of 8 well differentiated, 10

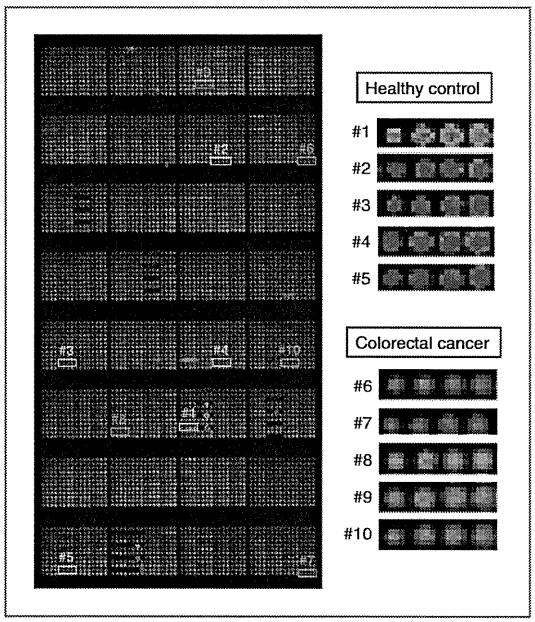

Figure 2. Representative reverse-phase protein microarray slide of the V1 cohort stained with anti-ADFP antibody (left). Magnified images of quadruplicate spots of representative individuals with high and low levels of adipophilin (right).

moderately differentiated, and 2 poorly differentiated adenocarcinomas. A total of 14 of 20 cancer tissues from the well- and moderately differentiated cases showed positive staining for adipophilin, but neither of the 2 poorly differentiated samples was positive. In a majority of the well- and moderately differentiated tumors, strong staining for adipophilin was observed in the cytoplasm or cell membrane of tumor glands facing the basement membrane (Fig. 4A and B). Adipophilin was not expressed in normal epithelial cells of the colorectal mucosa (Fig. 4C). The expression of adipophilin was clearly diminished in cancer cells invading in a scattered manner (Fig. 4D), which is consistent with the lack of staining observed in poorly differentiated tumor samples.

Discussion

In this study, we first enriched the LMW plasma protein fraction using HFMT, then compared its contents between patients with colorectal cancer and healthy controls using 2DICAL (Fig. 1). The high efficacy of combining HFMT and 2DICAL for plasma biomarker discovery was shown for the first time in our previous study of pancreatic cancer (17), and the present results further strengthened the credible evidence for the applicability of this combination of methods to all types of future plasma biomarker research. Any biomarker candidate identified by proteomic approaches must be validated using a different

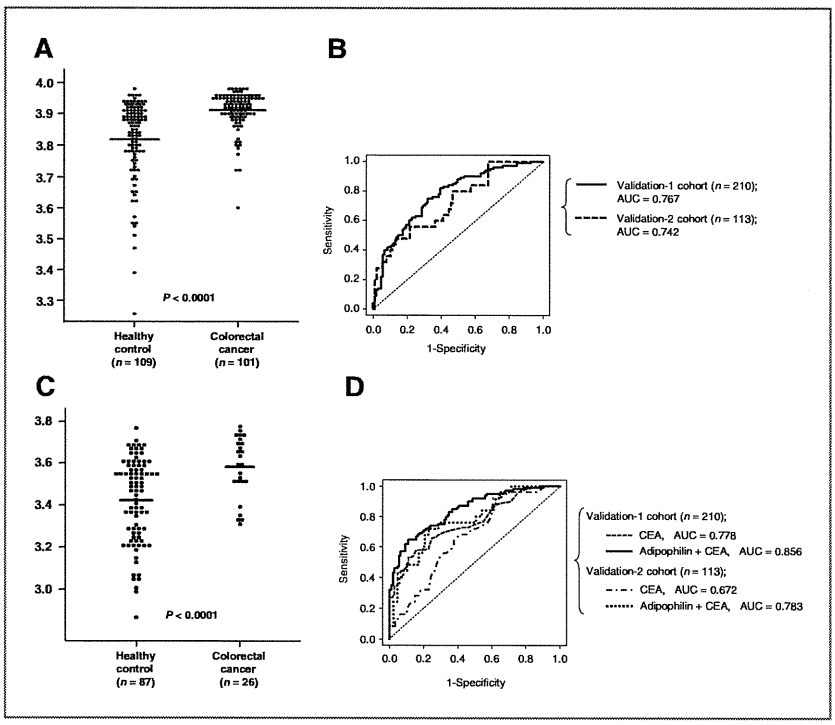

Figure 3. A and C, plasma adipophilin level in healthy controls and patients with colorectal cancer in the V1 (A) and V2 (C) cohorts. Horizontal lines represent the average adipophilin level. B, ROC analyses illustrating the discriminatory capability of adipophilin in the V1 (solid line) and V2 (dashed line) cohorts. D, ROC analyses illustrating the discriminatory value of CEA and the composite index of adipophilin and CEA in the V1 and V2 cohorts.

Table 2. Plasma adipophilin and CEA levels according to clinical stage of colorectal cancer [UICC TNM classification of malignant tumors, 6th edition (2002)] in the V1 cohort

	Colorectal cancer patients				Healthy controls
	Stage I	**Stage II**	**Stage III**	**Stage IV**	
No. of cases	19	31	32	17	109
Adipophilin[a], mean (SD)	3.90 (0.05)	3.91 (0.07)	3.91 (0.07)	3.93 (0.03)	3.82 (0.13)
P^b (vs. healthy controls)	1.07×10^{-5}	3.31×10^{-6}	1.65×10^{-6}	2.27×10^{-11}	Ð
CEA, mean (SD), ng/mL	2.63 (1.71)	13.7 (36.2)	224 (1,068)	200 (579)	2.07 (1.74)
P^b (vs. healthy controls)	0.20	0.09	0.25	0.18	Ð

[a]Measured using a reverse-phase protein microarray (values were transformed into logarithmic variables).
[b]Welch's *t* test (comparison with healthy controls).

method in a statistically sufficient number of cases and controls before it can be considered for clinical application. We employed another innovative technology, a reverse-phase protein microarray, for independent validation of our finding that adipophilin discriminates colorectal cancer (Fig. 2). Our high-density protein microarray enabled the high-throughput quantification of 1 protein in hundreds of clinical samples in 1 experiment (18), while keeping the required volume of each sample to a minimum (nanoliter level). Although the availability of clinical samples is often limited, it is often necessary to waste hundreds of microliters of samples for preliminary experiments involving techniques such as conventional ELISA. Because of their minimal sample requirements, plasma microarrays are considered to be ideal alternatives to ELISAs for biomarker validation. However, the absolute concentration and optimal cut-off value of adipophilin were not determined in this study. It may be necessary to establish an ELISA prior to the clinical application of the present results.

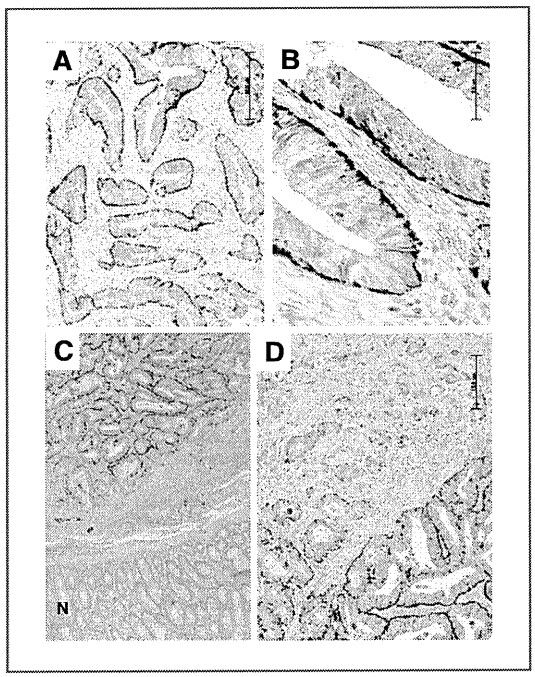

Figure 4. Immunohistochemical analysis of adipophilin in colorectal cancer (A–D) and adjacent normal colonic mucosa (designated by N; C). Original magnification; A and D = 100×; B = 400×; C = 40×.

Although the expression of adipophilin is known to be induced in various types of pathologic and physiologic conditions, such as lactating mammary epithelial cells, few studies have assessed the significance of its expression in cancer cells (27, 28). We found that adipophilin is expressed in well- or moderately differentiated adenocarcinomas, but not in the adjacent normal colonic mucosa or poorly differentiated adenocarcinoma (Fig. 4). The immunohistochemical data suggest that the expression of adipophilin is induced during the process of early colorectal carcinogenesis but lost during the process of cancer promotion. Consistent with our findings, Yao and colleagues also reported that adipophilin expression correlates well with the differentiation status of clear cell renal carcinoma of the kidney (29). They also reported that adipophilin expression is a prognostic factor for the cancer-specific survival of patients with renal clear cell carcinoma (29). The prognostic significance of adipophilin expression in colorectal cancer, however, remains to be determined.

The expression of adipophilin is known to be regulated by hypoxia inducible factor (HIF) and the peroxisome proliferator-activated receptor (PPAR) family of proteins. Both HIF and PPAR were reported to be closely involved in carcinogenesis, especially in colorectal cancer (30, 31). Moreover, PPARγ may be a molecular target of anticancer therapy (32). Because the exact nature of the interactions between these proteins (adipophilin, HIF, and PPAR) has not been extensively investigated, further studies are needed to elucidate the biological and clinicopathologic significance of adipophilin expression in colorectal

cancer. The present findings may provide novel insights into the molecular mechanism of colorectal cancer development and progression and into the development of new anticancer therapeutics.

There are some limitations to our study. First, we have no data about the body mass index of cases included in this study. The relationship between obesity and an increased risk of colon cancer is now generally accepted (33–35), and alteration of adipocytokine levels can reportedly affect intestinal carcinogenesis (36). Although adipophilin was originally identified as a marker of adipocyte development (27, 37), its relevance to body shape and cachexia remain to be elucidated. Adipophilin is a 50 kDa protein belonging to the PAT family (perilipin, adipophilin, TIP47, S3-12, and OXPAT), which comprises proteins involved in the coating of lipid droplets (27, 38, 39). Second, we have no data of FOB test results for the cases used in this study and thus it was not possible to show the superiority of adipophilin to FOB. However, a recent large-scale study showed that 11% of patients with negative FOB results had cancers or adenomas that required treatment (40). Because the adipophilin level was significantly elevated, even in patients with localized early colorectal cancer (Table 2), adipophilin may supplement or surpass the diagnostic power of FOB. Finally, there was a difference in the age distribution between cancer and control in all cohorts. However, age did not correlate with plasma adipophilin level in the cancer and control group (Pearson's $r = 0.03$ and $r = 0.09$, respectively). We therefore estimate the influence of difference in age to be negligible.

In conclusion, we identified plasma adipophilin as a new tumor marker for colorectal cancer using LMW protein profiling. The increase of plasma adipophilin level in colorectal cancer was validated in 2 larger cohorts, and the diagnostic power was revealed to be superior to that of CEA in the detection of early-stage (stages I and II) colorectal cancer. To our knowledge, this is the first study showing the expression of adipophilin in colorectal cancer. While bearing the above limitations in mind, an independent validation study is warranted.

Disclosure of Potential Conflicts of Interest

The sponsors of the study had no role in the design of the study, data collection, data analysis and interpretation, the decision to submit the manuscript for publication, or the writing of the manuscript.

Acknowledgments

We thank Ms. Ayako Igarashi, Ms. Tomoko Umaki, and Ms. Yuka Nakamura for their technical assistance.

Grant Support

This study was supported by the "Program for Promotion of Fundamental Studies in Health Sciences" conducted by the National Institute of Biomedical Innovation of Japan, the "Third-Term Comprehensive Control Research for Cancer" and "Research on Biological Markers for New Drug Development" conducted by the Ministry of Health and Labor of Japan.

The costs of publication of this article were defrayed in part by the payment of page charges. This article must therefore be hereby marked *advertisement* in accordance with 18 U.S.C. Section 1734 solely to indicate this fact.

Received April 27, 2011; revised July 12, 2011; accepted August 1, 2011; published OnlineFirst August 9, 2011.

References

1. Jemal A, Siegel R, Ward E, Hao Y, Xu J, Murray T, et al. Cancer statistics, 2008. CA Cancer J Clin 2008;58:71–96.
2. Ministry of Health, Labour and Welfare. Japanese Government: Vital Statistics of Japan. 2009; http://ganjoho.ncc.go.jp/professional/statistics/odjrh3000000hwsa-att/cancer_mortality(1958-2008).xls.
3. Andre T, Boni C, Navarro M, Tabernero J, Hickish T, Topham C, et al. Improved overall survival with oxaliplatin, fluorouracil, and leucovorin as adjuvant treatment in stage II or III colon cancer in the MOSAIC trial. J Clin Oncol 2009;27:3109–16.
4. Wolmark N, Yothers G, O'Connell MJ, Sharif S, Atkins JN, Seay TE, et al. A phase III trial comparing mFOLFOX6 to mFOLFOX6 plus bevacizumab in stage II or III carcinoma of the colon: Results of NSABP Protocol C-08. J Clin Oncol 2009;27: abstr LBA4.
5. Tol J, Koopman M, Cats A, Rodenburg CJ, Creemers GJ, Schrama JG, et al. Chemotherapy, bevacizumab, and cetuximab in metastatic colorectal cancer. N Engl J Med 2009;360:563–72.
6. Mandel JS, Bond JH, Church TR, Snover DC, Bradley GM, Schuman LM, et al. Reducing mortality from colorectal cancer by screening for fecal occult blood. Minnesota Colon Cancer Control Study. N Engl J Med 1993;328:1365–71.
7. Kronborg O, Fenger C, Olsen J, Jorgensen OD, Sondergaard O. Randomised study of screening for colorectal cancer with faecal-occult-blood test. Lancet 1996;348:1467–71.
8. Hardcastle JD, Chamberlain JO, Robinson MH, Moss SM, Amar SS, Balfour TW, et al. Randomised controlled trial of faecal-occult-blood screening for colorectal cancer. Lancet 1996;348:1472–7.
9. Greenberg PD, Bertario L, Gnauck R, Kronborg O, Hardcastle JD, Epstein MS, et al. A prospective multicenter evaluation of new fecal occult blood tests in patients undergoing colonoscopy. Am J Gastroenterol 2000;95:1331–8.
10. van Rossum LG, van Rijn AF, Laheij RJ, van Oijen MG, Fockens P, van Krieken HH, et al. Random comparison of guaiac and immunochemical fecal occult blood tests for colorectal cancer in a screening population. Gastroenterology 2008;135:82–90.
11. Locker GY, Hamilton S, Harris J, Jessup JM, Kemeny N, Macdonald JS, et al. ASCO 2006 update of recommendations for the use of tumor markers in gastrointestinal cancer. J Clin Oncol 2006;24:5313–27.
12. Yamaguchi U, Nakayama R, Honda K, Ichikawa H, Hasegawa T, Shitashige M, et al. Distinct gene expression-defined classes of gastrointestinal stromal tumor. J Clin Oncol 2008;26:4100–8.
13. Ono M, Shitashige M, Honda K, Isobe T, Kuwabara H, Matsuzuki H, et al. Label-free quantitative proteomics using large peptide data sets generated by nanoflow liquid chromatography and mass spectrometry. Mol Cell Proteomics 2006;5:1338–47.
14. Matsubara J, Ono M, Negishi A, Ueno H, Okusaka T, Furuse J, et al. Identification of a predictive biomarker for hematologic toxicities of gemcitabine. J Clin Oncol 2009;27:2261–8.
15. Negishi A, Ono M, Handa Y, Kato H, Yamashita K, Honda K, et al. Large-scale quantitative clinical proteomics by label-free liquid chromatography and mass spectrometry. Cancer Sci 2009;100:514–9.
16. Ono M, Matsubara J, Honda K, Sakuma T, Hashiguchi T, Nose H, et al. Prolyl 4-hydroxylation of alpha-fibrinogen: a novel protein modification revealed by plasma proteomics. J Biol Chem 2009;284:29041–9.
17. Matsubara J, Honda K, Ono M, Tanaka Y, Kobayashi M, Jung G, et al. Reduced plasma level of CXC chemokine ligand 7 in patients with

pancreatic cancer. Cancer Epidemiol Biomarkers Prev 2011;20: 160–71.
18. Matsubara J, Ono M, Honda K, Negishi A, Ueno H, Okusaka T, et al. Survival prediction for pancreatic cancer patients receiving gemcitabine treatment. Mol Cell Proteomics 2010;9:695–704.
19. Kennedy S. The role of proteomics in toxicology: identification of biomarkers of toxicity by protein expression analysis. Biomarkers 2002;7:269–90.
20. Tirumalai RS, Chan KC, Prieto DA, Issaq HJ, Conrads TP, Veenstra TD. Characterization of the low molecular weight human serum proteome. Mol Cell Proteomics 2003;2:1096–103.
21. Anderson NL, Anderson NG. The human plasma proteome: history, character, and diagnostic prospects. Mol Cell Proteomics 2002;1: 845–67.
22. Tanaka Y, Akiyama H, Kuroda T, Jung G, Tanahashi K, Sugaya H, et al. A novel approach and protocol for discovering extremely low-abundance proteins in serum. Proteomics 2006;6:4845–55.
23. http://www.fhcrc.org/science/international_biomarker/.
24. Honda K, Yamada T, Hayashida Y, Idogawa M, Sato S, Hasegawa F, et al. Actinin-4 increases cell motility and promotes lymph node metastasis of colorectal cancer. Gastroenterology 2005;128:51–62.
25. Idogawa M, Yamada T, Honda K, Sato S, Imai K, Hirohashi S. Poly (ADP-ribose) polymerase-1 is a component of the oncogenic T-cell factor-4/beta-catenin complex. Gastroenterology 2005;128:1919–36.
26. Carpelan-Holmstrom M, Louhimo J, Stenman UH, Alfthan H, Jarvinen H, Haglund C. Estimating the probability of cancer with several tumor markers in patients with colorectal disease. Oncology 2004;66: 296–302.
27. Heid HW, Moll R, Schwetlick I, Rackwitz HR, Keenan TW. Adipophilin is a specific marker of lipid accumulation in diverse cell types and diseases. Cell Tissue Res 1998;294:309–21.
28. de Wilde J, Smit E, Snepvangers FJ, de Wit NW, Mohren R, Hulshof MF, et al. Adipophilin protein expression in muscle–a possible protective role against insulin resistance. FEBS J 2010;277:761–73.
29. Yao M, Huang Y, Shioi K, Hattori K, Murakami T, Nakaigawa N, et al. Expression of adipose differentiation-related protein: a predictor of cancer-specific survival in clear cell renal carcinoma. Clin Cancer Res 2007;13:152–60.
30. Paul SA, Simons JW, Mabjeesh NJ. HIF at the crossroads between ischemia and carcinogenesis. J Cell Physiol 2004;200:20–30.
31. Osawa E, Nakajima A, Wada K, Ishimine S, Fujisawa N, Kawamori T, et al. Peroxisome proliferator-activated receptor gamma ligands suppress colon carcinogenesis induced by azoxymethane in mice. Gastroenterology 2003;124:361–7.
32. Grommes C, Landreth GE, Heneka MT. Antineoplastic effects of peroxisome proliferator-activated receptor gamma agonists. Lancet Oncol 2004;5:419–29.
33. Pischon T, Lahmann PH, Boeing H, Friedenreich C, Norat T, Tjonneland A, et al. Body size and risk of colon and rectal cancer in the European Prospective Investigation Into Cancer and Nutrition (EPIC). J Natl Cancer Inst 2006;98:920–31.
34. Giovannucci E, Michaud D. The role of obesity and related metabolic disturbances in cancers of the colon, prostate, and pancreas. Gastroenterology 2007;132:2208–25.
35. Renehan AG, Tyson M, Egger M, Heller RF, Zwahlen M. Body-mass index and incidence of cancer: a systematic review and meta-analysis of prospective observational studies. Lancet 2008;371: 569–78.
36. Mutoh M, Teraoka N, Takasu S, Takahashi M, Onuma K, Yamamoto M, et al. Loss of adiponectin promotes intestinal carcinogenesis in Min and wild-type mice. Gastroenterology 2011;140:2000–8.
37. Brasaemle DL. Thematic review series: adipocyte biology. The perilipin family of structural lipid droplet proteins: stabilization of lipid droplets and control of lipolysis. J Lipid Res 2007;48:2547–59.
38. Jiang HP, Serrero G. Isolation and characterization of a full-length cDNA coding for an adipose differentiation-related protein. Proc Natl Acad Sci U S A 1992;89:7856–60.
39. Martin S, Parton RG. Lipid droplets: a unified view of a dynamic organelle. Nat Rev Mol Cell Biol 2006;7:373–8.
40. Johnson CD, Chen MH, Toledano AY, Heiken JP, Dachman A, Kuo MD, et al. Accuracy of CT colonography for detection of large adenomas and cancers. N Engl J Med 2008;359:1207–17.

LEGEND FOR SUPPLEMENTARY FIGURE

Supplementary Figure S1 (online).

MS/MS spectra and database search result for a single MS peak (ID 83) derived from adipophilin. The adipophilin peptide matching the amino acid sequence in the database is highlighted in red (*bottom*).

LIST OF TABLES

Supplementary Table S1 (online).

Plasma Proteins for which the MS Peak Intensity Differed Significantly between Healthy Controls and Patients with Colorectal Cancer.

Supplementary Figure S1

Peak ID: 83

MS/MS Fragmentation of **EMAENGV**
Found in **ADFP_HUMAN**, Adipophilin (Adipose differentiation-related protein) (ADRP) - Homo sapiens (Human)
Match to Query 2: 748.347984 from(749.355260,1+)

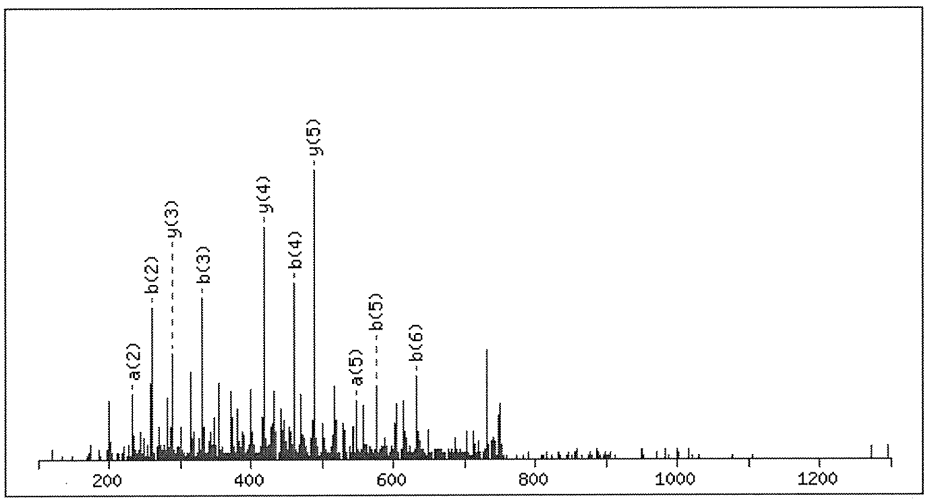

Monoisotopic mass of neutral peptide Mr(calc): 748.3061
Ions Score: 44 Expect: 0.21
Matches (Bold Red): 10/26 fragment ions using 25 most intense peaks

#	a	a*	b	b*	Seq.	y	y*	#
1	102.0550		130.0499		E			7
2	**233.0954**		**261.0904**		M	620.2708	603.2443	6
3	304.1326		**332.1275**		A	**489.2304**	472.2038	5
4	433.1751		**461.1701**		E	**418.1932**	401.1667	4
5	**547.2181**	530.1915	**575.2130**	558.1864	N	**289.1506**	272.1241	3
6	604.2395	587.2130	**632.2345**	615.2079	G	175.1077		2
7					V	118.0863		1

Matched peptides shown in Bold Red

```
  1 MASVAVDPQP SVVTRVVNLP LVSSTYDLMS SAYLSTKDQY PYLKSVCEMA
 51 ENGVKTITSV AMTSALPIIQ KLEPQIAVAN TYACKGLDRI EERLPILNQP
101 STQIVANAKG AVTGAKDAVT TTVTGAKDSV ASTITGVMDK TKGAVTGSVE
151 KTKSVVSGSI NTVLGSRMMQ LVSSGVENAL TKSELLVEQY LPLTEEELEK
201 EAKKVEGFDL VQKPSYYVRL GSLSTKLHSR AYQQALSRVK EAKQKSQQTI
251 SQLHSTVHLI EFARKNVYSA NQKIQDAQDK LYLSWVEWKR SIGYDDTDES
301 HCAEHIESRT LAIARNLTQQ LQTTCHTLLS NIQGVPQNIQ DQAKHMGVMA
351 GDIYSVFRNA ASFKEVSDSL LTSSKGQLQK MKESLDDVMD YLVNNTPLNW
401 LVGPFYPQLT ESQNAQDQGA EMDKSSQETQ RSEHKTH
```

Supplementary Table S1. Plasma Proteins for which the MS Peak Intensity Differed Significantly Between Healthy Controls and Patients with Colorectal Cancer

Gene locus	Protein identification	Mascot score	AUC	Matched peptide
HBD_HUMAN	Hemoglobin subunit delta (Hemoglobin delta chain) (Delta-globin) - Homo sapiens (Human)	90.18	0.86	1
HBB_HUMAN	Hemoglobin subunit beta (Hemoglobin beta chain) (Beta-globin) - Homo sapiens (Human)	74.50	0.82	5
RETBP_HUMAN	Plasma retinol-binding protein precursor (PRBP) (RBP) [Contains: Plasma retinol-binding protein (1-182); Plasma retinol-binding protein (1-181); Plasma retinol-binding protein (1-179); Plasma retinol-binding protein (1-176)] - Homo sapiens (Human)	66.52	0.82	1
HBA_HUMAN	Hemoglobin subunit alpha (Hemoglobin alpha chain) (Alpha-globin) - Homo sapiens (Human)	63.75	0.81	2
ADFP_HUMAN	Adipophilin (Adipose differentiation-related protein) (ADRP) - Homo sapiens (Human)	43.67	0.81	1
PKDRE_HUMAN	Polycystic kidney disease and receptor for egg jelly-related protein precursor (PKD and REJ homolog) - Homo sapiens (Human)	41.62	0.81	1

NOTE. *Peaks with a Mascot score >40.

Hindawi Publishing Corporation
International Journal of Proteomics
Volume 2011, Article ID 739615, 11 pages
doi:10.1155/2011/739615

Research Article

Combined Use of a Solid-Phase Hexapeptide Ligand Library with Liquid Chromatography and Two-Dimensional Difference Gel Electrophoresis for Intact Plasma Proteomics

Tatsuo Hagiwara,[1,2] Yumi Saito,[1] Yukiko Nakamura,[1,3] Takeshi Tomonaga,[3] Yasufumi Murakami,[2] and Tadashi Kondo[1]

[1] *Division of Pharmacoproteomics, National Cancer Center Research Institute, Chuo-ku, Tokyo 104-0045, Japan*
[2] *Laboratory of Genome Biology, Department of Biological Science and Technology, Tokyo University of Science, Tokyo 278-8510, Japan*
[3] *Laboratory of Proteome Research, National Institute of Biomedical Innovation, Osaka 567-0085, Japan*

Correspondence should be addressed to Tadashi Kondo, takondo@ncc.go.jp

Received 2 May 2011; Accepted 9 June 2011

Academic Editor: David E. Misek

The intact plasma proteome is of great interest in biomarker studies because intact proteins reflect posttranslational protein processing such as phosphorylation that may correspond to disease status. We examined the utility of a solid-phase hexapeptide ligand library in combination with conventional plasma proteomics modalities for comprehensive profiling of intact plasma proteins. Plasma proteins were sequentially fractionated using depletion columns for albumin and immunoglobulin, and separated using an anion-exchange column. Proteins in each fraction were treated with a solid-phase hexapeptide ligand library and compared to those without treatment. Two-dimensional difference gel electrophoresis demonstrated an increased number of protein spots in the treated samples. Mass spectrometric studies of these protein spots with unique intensity in the treated samples resulted in the identification of high- and medium-abundance proteins. Our results demonstrated the possible utility of a solid-phase hexapeptide ligand library to reveal greater number of intact plasma proteins. The characteristics of proteins with unique affinity to the library remain to be clarified by more extensive mass spectrometric protein identification, and optimized protocols should be established for large-scale plasma biomarker studies.

1. Introduction

The plasma proteome has been extensively investigated with the aim of biomarker development [1, 2]. Plasma is the most accessible clinical material, and plasma biomarkers for early diagnosis and monitoring the response to therapy and disease recurrence would be beneficial for patients with cancer. Because proteins released by tumors, particularly early-stage tumors, are expected to exist in very low concentrations and plasma contains various proteins with considerable heterogeneity between and within patients, the identification of novel plasma biomarkers represents a substantial challenge.

Global expression studies on intact plasma proteins are of special interest in biomarker studies as the intact proteins reflect the functional features of protein structure. Those include posttranslational processing such as phosphorylation and glycosylation. Peptide subsets from complex digests have been analyzed for plasma proteomics, resulting in the identification of low-abundance proteins such as tissue leakage proteins [3] and biomarker candidates [4]. However, analysis of peptide digests may not be sensitive to posttranslational protein processing, and may therefore not reveal many relevant protein isoforms associated with disease status. To date, much effort has been devoted to detect trace intact proteins in complex plasma samples.

The utility of a combinatorial hexapeptide ligand library immobilized on a solid-phase matrix has been reported, introduced to intact plasma proteomics [5–9], and

commercialized as ProteoMiner (Bio-Rad Laboratories, Hercules, CA, USA). ProteoMiner contains millions of randomly synthesized hexapeptide ligands that are equally represented with a selected number of targets. When a complex plasma protein extract is exposed, the hexapeptide ligands for high-abundance proteins are saturated, but the majority remains unbound. In contrast, the proteins which do not saturate the corresponding hexapeptide ligands and usually not observed by the conventional methods will appear in the proteome data. The approach of using a combinatorial hexapeptide ligand library is different from that of using depletion and separation; thus, it reveals a novel aspect of the plasma proteome. A recent report demonstrated that prefractionation using a hexapeptide ligand library for shotgun mass spectrometry studies identified plasma proteins not recorded in the Human Plasma Proteome Project [10]. The combined use of a hexapeptide ligand library with depletion and separation methods has also been a challenge in deeper plasma proteomics [11], and the resulting protein contents are examined by gel electrophoresis and mass spectrometry [12, 13]. ProteoMiner has been used for disease biomarker studies in lung cancer [14] and liver cancer [15]. Considering that it will potentially visualize the unique plasma proteome aspects, the application and optimization of a solid-phase hexapeptide ligand library for disease biomarker studies should be further investigated.

In this study, we examined the utility of a solid-phase hexapeptide ligand library in combination with a depletion column, an anion-exchange column, and 2D-DIGE that allows an instant visual comparison of the protein patterns. Protein spots exhibiting prominent differences between samples treated with and without the library were subjected to mass spectrometry. Our study clearly demonstrated that the combined use of the ProteoMiner and the other proteomics modalities can visualize unique plasma proteome.

2. Materials and Methods

2.1. Sample Preparation. Frozen human plasma was purchased from Cosmobio KOJ (Tokyo, Japan). After the plasma was placed on ice, 40 mL plasma was centrifuged and 30 mL supernatant was recovered for the following experiments.

2.2. Albumin Depletion. Albumin and other proteins were separated using a HiTrap Blue HP column (5 mL resin, GE, Uppsala, Sweden) with the AKTA Explorer system (GE) at a flow rate of 1.0 mL/min. The separation was initiated by washing the column with rinse buffer (50 mM KH_2PO_4/Na_2HPO_4, pH 7.0) for 5 min. Plasma (30 mL) was diluted with 60 mL 50 mM KH_2PO_4/Na_2HPO_4 (pH 7.0), and 9 mL of the diluted plasma was injected. The column was then washed with binding buffer (50 mM KH_2PO_4/Na_2HPO_4, pH 7.0) for 35 min, and the flow-through fraction was collected. Bound proteins were eluted from the column with elution buffer (50 mM $KHPO_4$, 1.5 M KCl, pH 7.0) for 45 min, and the bound fraction was collected. The column was neutralized with rinse buffer for 20 min. This process was repeated 10 times for a total of 90 mL of diluted plasma.

One-third of the flow-through and bound fractions, approximately 150 mL of each, was concentrated to 1.2 mL using a VIVA Spin 20 column (10 K MWCO, 20 mL capacity, Sartorius, Gotteingen, Germany). Then, 1.0 mL and 0.20 mL of the concentrated samples were subjected to treatment with the solid-phase hexapeptide ligand library and 2D-DIGE, respectively. Two-thirds of the flow-through fraction, approximately 300 mL, was subjected to an immunodepletion column.

2.3. Immunoglobulin Depletion. Immunoglobulin was depleted using the HiTrap Protein G HP column (1 mL resin, GE) with the AKTA Explorer system (GE) at a flow rate of 1.0 mL/min. The depletion was initiated by washing the column with rinse buffer (50 mM KH_2PO_4/Na_2HPO_4, pH 7.0) for 4 min. After 15 mL of the flow-through fraction from the HiTrap Blue HP column was injected, the column was washed with binding buffer (50 mM KH_2PO_4/Na_2HPO_4, pH 7.0) for 5 min, and the flow-through fraction was collected. Bound proteins were eluted from the column with elution buffer (0.1 M glycine-HCl, pH 2.2) for 8 min and collected as the bound fraction. The collected bound fraction was immediately neutralized with neutralizing buffer (1.0 M Tris-HCl, pH 9.0). The column was equilibrated with rinse buffer for 5 min for reuse. This process was repeated 20 times for a total of two-thirds of the flow-through fraction from the HiTrap Blue HP column (approximately 300 mL).

Half of the flow-through and bound fractions (approximately 200 mL and 80 mL, resp.) were concentrated to 1.2 mL and 0.25 mL, respectively, using VIVA Spin 20 columns (Sartorius). Then, 1.0 mL of the concentrated flow-through fraction and 0.20 mL of the concentrated bound fraction were subjected to treatment with the solid-phase ligand library, and the remaining samples were subjected to 2D-DIGE. Another half of the flow-through fraction (approximately 200 mL) was concentrated to 2.0 mL using the VIVA Spin 20 column (Sartorius). After diluting with 38 mL of 25 mM Tris-HCl (pH 9.0), the sample was subjected to separation on an anion-exchange column.

2.4. Anion Exchange. The flow-through fraction from the HiTrap Protein G HP column was separated using the Resource Q column (1 mL resin, 6.4 mm id × 30 mm, GE) with the AKTA Explorer system (GE) at a flow rate of 3.0 mL/min. The separation was initiated by washing the column with rinse buffer (25 mM Tris-HCl, pH 9.0) for 4 min, and 5 mL of the flow-through fraction from the HiTrap Protein G HP column was injected. The separations were performed using a stepwise NaCl gradient as follows: 0, 100, 150, 200, 250, and 1000 mM for 5 min each. All samples contained 25 mM Tris-HCl, pH 9.0. The column was washed with rinse buffer (25 mM Tris-HCl, pH 9.0) for 5 min. This process was repeated 8 times for a total of 40 mL of the diluted flow-through fraction from the HiTrap Protein G HP column.

The collected samples were concentrated to 0.25 mL, and the buffer was exchanged gradually with 25 mM Tris-HCl (pH 9.0) using the VIVA Spin 20 column (Sartorius). Then,

0.2 mL and 0.05 mL were subjected to treatment with the solid-phase ligand library and 2D-DIGE, respectively.

2.5. Treatment with the Solid-Phase Ligand Library. A solid-phase combinatorial library of hexapeptides was purchased from Bio-Rad Laboratories (ProteoMiner kit). Unprocessed plasma (1 mL) and the flow-through fractions from the HiTrap Blue HP and HiTrap Protein G HP columns were treated using the ProteoMiner large-capacity kit, and 0.2 mL of the bound fraction from the HiTrap Protein G HP column, and all fractions from the Resource Q column were treated using the ProteoMiner small-capacity kit. After 2 h of incubation at room temperature, the unbound fraction was washed out by centrifugation. After rinsing, the bound sample was eluted with an elution reagent containing 8 M urea, 2% CHAPS, and 5% acetic acid, according to the manufacturer's instructions.

2.6. Measurement of Protein Concentration. Protein concentration was measured using a protein assay kit (Bio-Rad), according to the manufacturer's instructions (Table 1).

2.7. SDS-PAGE. Protein samples (1 μg) were examined by electrophoresis using 18-well precast 12.5% polyacrylamide gel plates (e-PAGEL, ATTO, Tokyo, Japan). Electrophoresis was performed at a constant current of 40 mA for 80 min and using the page Run AE6531 system [16]. Silver staining was performed using the Silver Stain KANTO III kit (Kanto Chemical, Tokyo, Japan), according to the manufacturer's instructions.

2.8. 2D-DIGE. 2D-DIGE was performed as described previously [17]. Briefly, protein samples (20 μg) were labeled with the Cy3 or Cy5 fluorescent dye (CyDye DIGE Fluor saturation dye, GE), and differentially labeled protein samples were mixed. After dividing into 3, the labeled protein samples were separated by 2D-PAGE. The first-dimension separation was performed using a 24 cm length immobiline gel (IPG, pI 4–7, GE) and Multiphor II (GE) whereas the second-dimension separation was performed using gradient gels prepared in house and EttanDalttwelve (GE). The gels were scanned using a laser scanner (Typhoon Trio, GE) at an appropriate wavelength for Cy3 or Cy5. The Cy3 and Cy5 intensities were compared in the same gel using the Progenesis SameSpots software (version 4.0; Nonlinear Dynamics, Newcastle, UK). ProteoMiner-treated and untreated samples were labeled with Cy3 and Cy5, respectively, or with Cy5 and Cy3, respectively. Six gels were run for each sample. The average value of the intensity ratio was calculated among the triplicate gels for all protein spots and then averaged between the 2 samples for further study. Spot intensity data were exported from the Progenesis SameSpots software as Excel files amenable to numerical data analysis.

2.9. Mass Spectrometric Protein Identification. Proteins were extracted from the protein spots by in-gel digestion, as reported previously [17]. Briefly, protein samples (100 μg) were labeled with Cy3 and separated by 2D-PAGE. The protein spots were then recovered from the gel pieces using an automated spot recovery machine. The recovered protein spots were extensively washed with a solution containing acetonitrile and ammonium bicarbonate minimum and treated with trypsin (Promega, Madison, WI, USA) at 37°C overnight. The tryptic digests were recovered from the gel pieces, concentrated by vacuum, and resolubilized with 0.1% trifluoroacetic acid. The final tryptic digests were subjected to mass spectrometry, which was performed using the LXQ linear ion trap mass spectrometer (Thermo Electron, San Jose, CA, USA). The Mascot software (version 2.3.0; Matrix Science, London, UK) was used to search for the mass of the peptide ion peaks against the SWISS-PROT database (Homo sapiens, 471472 sequences in Sprot_57.5 fasta file). The search parameters were as follows: trypsin digestion allowing up to 3 missed tryptic cleavages, fixed modifications of

TABLE 1: List of the identified proteins and their reported concentration.

Protein name	Normal concentration μg/mL
Adiponectin	2–17
Albumin	35000–52000
Alpha-1-antitrypsin	900–2000
Alpha-1B-glycoprotein	150–300
Alpha-2-macroglobulin	1300–3000
Apolipoprotein A-I	1000–2000
Apolipoprotein A-II	190–300
Apolipoprotein A-IV	110–220
Apolipoprotein D	60–90
Apolipoprotein E	30–60
Carboxypeptidase N	30
Ceruloplasmin	190–370
Clusterin	250–420
Coagulation factor X	10
Complement C3	900–1800
Complement C4-A	25–90
Fibrinogen beta chain	520–1420
Fibrinogen gamma chain	490–1340
Ficolin-2	1–12
Ficolin-3	3–54
Haptoglobin	200–2000
Haptoglobin-related protein	32–41
Inter-alpha-trypsin inhibitor (heavy chain H3)	100–200
Paraoxonase/arylesterase 1	58–61
Prothrombin	100
Serotransferrin	2000–3600
Transthyretin	200–400
Vitronectin	240–530
Zinc-alpha-2-glycoprotein	60–80

The table with the references for the protein concentration is shown in Supplementary Table 7 in Supplemrntary material available online at doi: 10.1155/2011/39615.

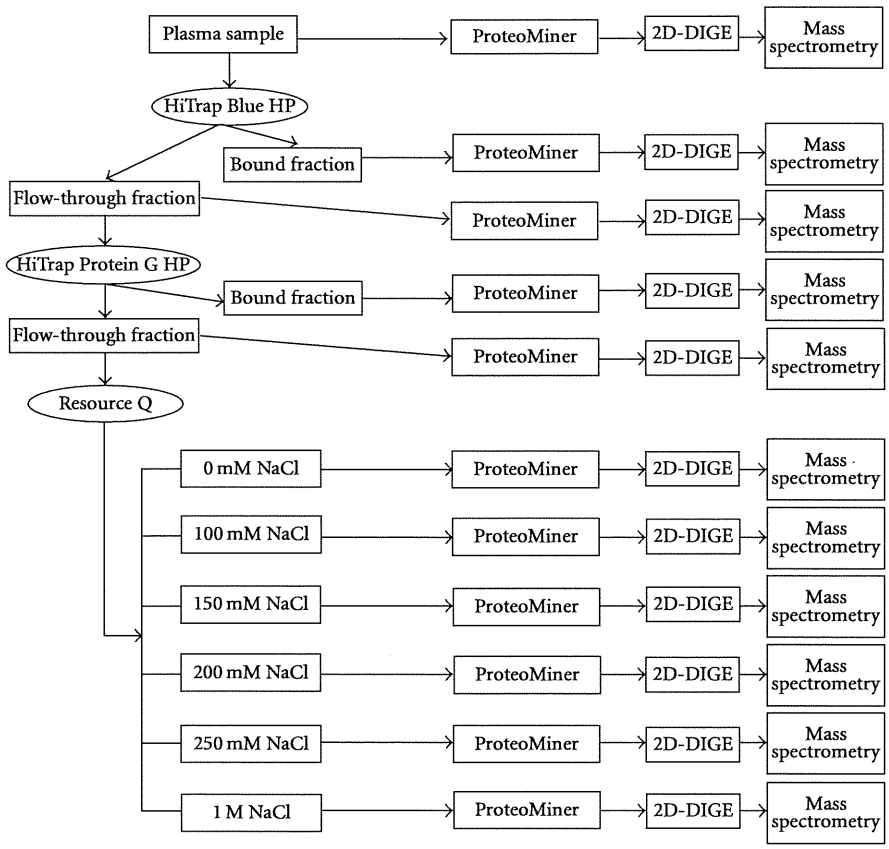

FIGURE 1: Overview of protein fractionation by sequential use of 3 different columns to separate plasma proteins. All fractions were subjected to ProteoMiner and 2D-DIGE.

carbamidomethyl, variable modifications of oxidation, 1^+, 2^+, and 3^+ peptide charge, peptide mass tolerance of 2.0 Da, and use of MS/MS tolerance of 1.0 Da for all tryptic-mass searches.

3. Results and Discussion

We previously reported the utility of combining multidimensional chromatography and 2D-DIGE for intact plasma proteomics. Extensive fractionation by the different separation modes increased the number of protein spots on 2D-DIGE and allowed a quantitative comparison between the plasma samples from healthy donors and those from patients with lung adenocarcinoma [18] and pancreatic cancer [19]. However, mass spectrometric protein identification revealed that protein spots with a significant difference between the sample groups corresponded to high- and medium-abundance proteins such as acute-phase proteins, but no known plasma tumor markers were detected. Thus, we concluded that further investigations are needed to reveal low-abundance proteins for biomarker studies. In this study, we examined whether a novel technology, a solid-phase hexapeptide ligand library could improve the linkage of multidimensional chromatography and 2D-DIGE.

3.1. Overall View of Protein Fractionation: Comparison and Detection. The overall view of sequential protein separation is shown in Figure 1. A sample equivalent to 10 mL plasma was separated using 3 different columns and then treated with the solid-phase hexapeptide ligand library ProteoMiner. The ProteoMiner-treated and untreated samples were compared using 2D-DIGE by labeling them with different fluorescent dyes and separating the labeled proteins on an identical gel. The protein spots with significantly different intensities between the ProteoMiner-treated and untreated samples were subjected to mass spectrometry to identify the proteins.

The number of observable low-abundance proteins was affected by the initial amount of plasma sample and the sensitivity of the final quantification method. We used a relatively large volume of plasma sample (10 mL) as the initial material. The immunodepletion columns allow the use of only a small volume of plasma sample for separation. Furthermore, a significantly larger number of plasma samples should be examined to obtain conclusive results for biomarker development. A larger volume of samples can be manipulated by repeatedly using the same immunodepletion column. Although it is quite feasible, special attention may be required to maintain reproducibility during a long period of use. In this study, we used Blue Sepharose and Protein

G-Sepharose columns in a sequential manner to deplete albumin and subsequently immunoglobulin and to minimize repeated use of the same column. Although these columns may have less sensitivity than an immunodepletion column and deplete nontargeted proteins that may bind to albumin and immunoglobulin, a larger volume of plasma sample can be treated in individual procedures. A previous study indicated that Cibacron Blue beads remove a major portion of the albumin but with concomitant loss of potentially important peptides and proteins [20]. Thus, we examined both the column-bound and flow-through fractions (Figure 1). Although the specificity of Cibacron Blue beads was not validated in this study, as the purpose of Cibacron Blue was to reduce the complexity of plasma sample, it should not be problem.

To avoid possible redundant proteins in the neighboring fractions as much as possible when utilizing the anion-exchange column, we used stepwise elution and fractionation; once all proteins were eluted, the next elution buffer was applied to the column (Figure 1). Considering the complexity of the samples and resolution of an anion-exchange column, extensive fractionation with a gradient buffer system may result in redundant contents among the fractions. We employed 6 stepwise fractionations by monitoring the fraction contents using SDS-PAGE (data not shown).

3.2. High Reproducibility of Protein Fractionation by Chromatography. The ultraviolet detection (280 nm) trace for each run demonstrated consistent separation of albumin and immunoglobulin from the depletion and anion-exchange columns. This high reproducibility may suggest the possible utilities of this approach for biomarker studies (Supplementary Figure 1). High quantitative and qualitative reproducibility of the solid-phase hexapeptide ligand library ProteoMiner has been confirmed in previous reports [21, 22].

3.3. Demonstration of the Effects of Fractionation and Dynamic Range Reduction. We examined the effects of sequential plasma protein fractionation using 3 columns and the reduction of dynamic range by ProteoMiner (Figure 2). The contents of the fractionated samples were apparently different from each other. Notably, the protein sample bound to the Blue Sepharose and Protein G-Sepharose columns included many proteins that should be different from the targeted proteins, according to their molecular weights. Treatment of the fractionated samples with ProteoMiner enhanced the proteins that were not observed, except for those bound to the Protein G-Sepharose column. Treatment of the bound fraction from the Protein G-Sepharose column with ProteoMiner did not result in a greater number of observable proteins. This may have been due to the low complexity and narrow dynamic range of proteins in the bound fraction from the Protein G-Sepharose column. There was one order of magnitude in concentration difference for the observed protein bands in the ProteoMiner-treated sample. These observations may reflect that the affinity of proteins for the peptide may not be equal and even the number of peptides bound on the beads is equal, the amount of proteins bound to the ProteoMiner may be different

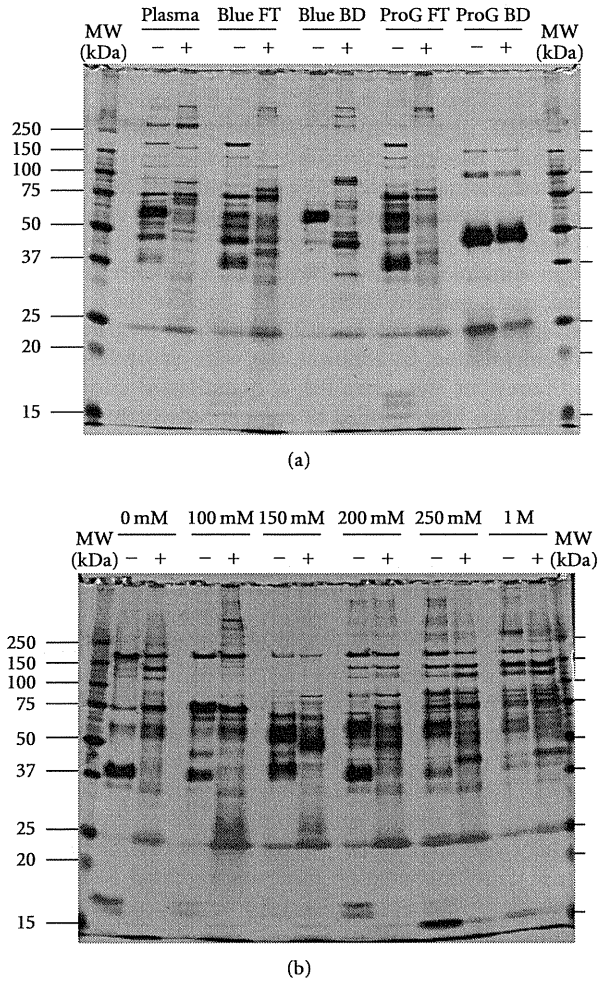

FIGURE 2: Overview of the protein contents fractionated by liquid chromatography and ProteoMiner. The fractionated protein samples were loaded onto SDS-PAGE, and the protein contents were visualized by silver staining.

depending on their affinity. This fraction contained similar amounts of only 4 major proteins, as revealed by SDS-PAGE (Figure 2), and they may have been absorbed to ProteoMiner in proportion to their original amount.

The concentration and amount of protein samples before and after ProteoMiner treatment are summarized in Supplementary Table 1. The recovery rate from ProteoMiner was between 0.54 and 6.33%, suggesting that a unique population of protein species selectively bound to ProteoMiner. This assumption was supported by the SDS-PAGE data, except the bound fraction from the Protein G-Sepharose column which included only 4 major proteins that were bound to ProteoMiner (Figure 2).

3.4. Higher Separation of Fractionated Protein Samples and an Evaluation of the Effects of ProteoMiner Treatment. Although SDS-PAGE separated individual proteins with higher

resolution than chromatography in this study, using it for a quantitative comparison in a biomarker study may be troublesome because many protein bands obviously overlapped (Figure 2). Thus, we subjected the fractionated samples to 2D-DIGE in order to separate the proteins with higher resolution. Bandow compared ProteoMiner-treated and untreated plasma samples using conventional 2D-PAGE and demonstrated substantial differences between unprocessed and immunodepleted plasma samples [11]. In 2D-DIGE, 2 protein samples were labeled with different fluorescent dyes, mixed, and separated by 2D-PAGE. Because the 2 samples were separated on an identical 2D-PAGE, gel-to-gel variation was compensated. In addition, the wide dynamic range of the fluorescent dyes enabled a quantitative comparison. 2D-DIGE has been applied to compare the performance of ProteoMiner with an immunodepletion column [12]. We further extended the evaluation of the utility of ProteoMiner by loading a high amount of protein and examining the proteins separated by an anion-exchange column.

The fluorescent 2D-PAGE images of the ProteoMiner-treated and untreated samples were overlaid with different colors, so that the unique protein contents were visualized (Figures 3 and 4). The results of experiments in which the fluorescent dyes were swapped are shown in Supplementary Figure 2. Consistent with the SDS-PAGE results (Figure 2), Figure 3 demonstrates that the approach involving depletion of high-abundance proteins and multidimensional separation was an effective prefractionation method to increase the number of protein spots, and the use of ProteoMiner treatment also contributed to reveal more plasma proteins. Because these fractionation methods are based on different binding properties of proteins, their combined use revealed additional plasma proteins.

The number of observed protein spots on 2D gel electrophoresis is summarized in Supplementary Table 2. Overall, the total number of protein spots increased by treating the samples with ProteoMiner, except for the bound fraction from the Protein G-Sepharose column. This observation suggests that ProteoMiner may be a useful tool to observe a greater number of protein spots in prefractionated samples.

We compared the protein spots of the samples with and without ProteoMiner treatment (Supplementary Table 3). Depending on the criteria, different numbers of protein spots showed significantly different intensities. Although the total number of protein spots increased by treating the samples with ProteoMiner (Supplementary Table 2), many protein spots revealed decreased intensity with treatment, suggesting the selective enrichment by ProteoMiner.

3.5. Mass Spectrometric Identification of Proteins with Different Affinities to ProteoMiner. To reveal the characteristics of proteins with a particularly high or low affinity to ProteoMiner, among the protein spots with greater than 5-fold differences (Supplementary Table 3), we selected those with the top 10% different intensities between the ProteoMiner-treated and untreated samples in each fraction and subjected them to mass spectrometric identification. A total of 200 protein spots were subjected to mass spectrometry, and a positive identification was obtained for 128 (Supplementary Table 4). A list of the identified proteins is provided in Supplementary Table 5, and data supporting protein identification are shown in Supplementary Table 6. These 128 protein spots corresponded to 29 unique proteins. Because the fold difference of the protein spots in the bound fraction from the Protein G-Sepharose column was less than 4, we did not examine them. Of the original plasma samples, vitronectin and albumin were most affected by ProteoMiner treatment and disappeared after depletion and fractionation using the anion-exchange column. The other proteins were identified as enriched (or nonenriched) by ProteoMiner treatment. Proteins bound to ProteoMiner have been reported in previous studies in which the proteins were globally identified by mass spectrometry. Dwivedi et al. demonstrated that albumin, alpha 1-antitrypsin, alpha 2-macroglobulin, apolipoprotein A-I, apolipoprotein A-II, haptoglobin-related protein, and serotransferrin have high affinity to ProteoMiner [21]. In addition, Beseme et al. identified apolipoprotein A-IV, apolipoprotein D, apolipoprotein E, ceruloplasmin, complement C3, fibrinogen beta, fibrinogen gamma, ficolin-2, ficolin-3, paroxonase I, prothrombin, transthyretin, and vitronectin [23]. The protein concentrations identified in this study are summarized in Supplementary Table 6. According to the literatures, the identified proteins were classified as high- and medium-abundance proteins. Adiponectin and the carboxypeptidase N catalytic chain are not reported in previous studies, in which ProteoMiner-treated samples were examined by 2D-PAGE and mass spectrometry.

Adiponectin is an adipocytokine [24–27] and plays a protective role against obesity-related disorders such as metabolic syndrome [28], type 2 diabetes [29], and cardiovascular disease [30]. Low levels of plasma adiponectin are associated with obesity [31] and many types of malignancies such as liver cancer [32], breast cancer [33], pancreatic cancer [34], and endometrial cancer [35]. An epidemiological study suggested that adiponectin is involved in early colorectal carcinogenesis [36], and that a low circulating adiponectin level is correlated with a poor prognosis in patients with colorectal cancer [37]. The molecular backgrounds of these observations may be attributable to the antiproliferative effects of adiponectin on cancer cells [38].

Carboxypeptidase N (CPN), which is also known as kininase I, arginine carboxypeptidase, and anaphylatoxin inactivator, is a zinc finger metalloprotease. It cleaves basic lysine and arginine residues from the carboxy terminal of proteins [39]. CPN is produced in the liver and secreted into the plasma. It modulates the activity of cytokines such as stromal cell-derived factor-1 alpha [40]. The association of CPN1 with malignancy and other diseases has not been reported, and the clinical utility of CPN1 has not been suggested.

The working hypothesis of this study was that the combined use of different separation methods, including a solid-phase hexapeptide ligand library, would increase the number of observable proteins, and finally visualize the proteome that may not be observed otherwise. By loading a high amount of protein and using extensive prefractionation techniques prior to using ProteoMiner, trace proteins became visible in SDS-PAGE, and the number of protein spots on

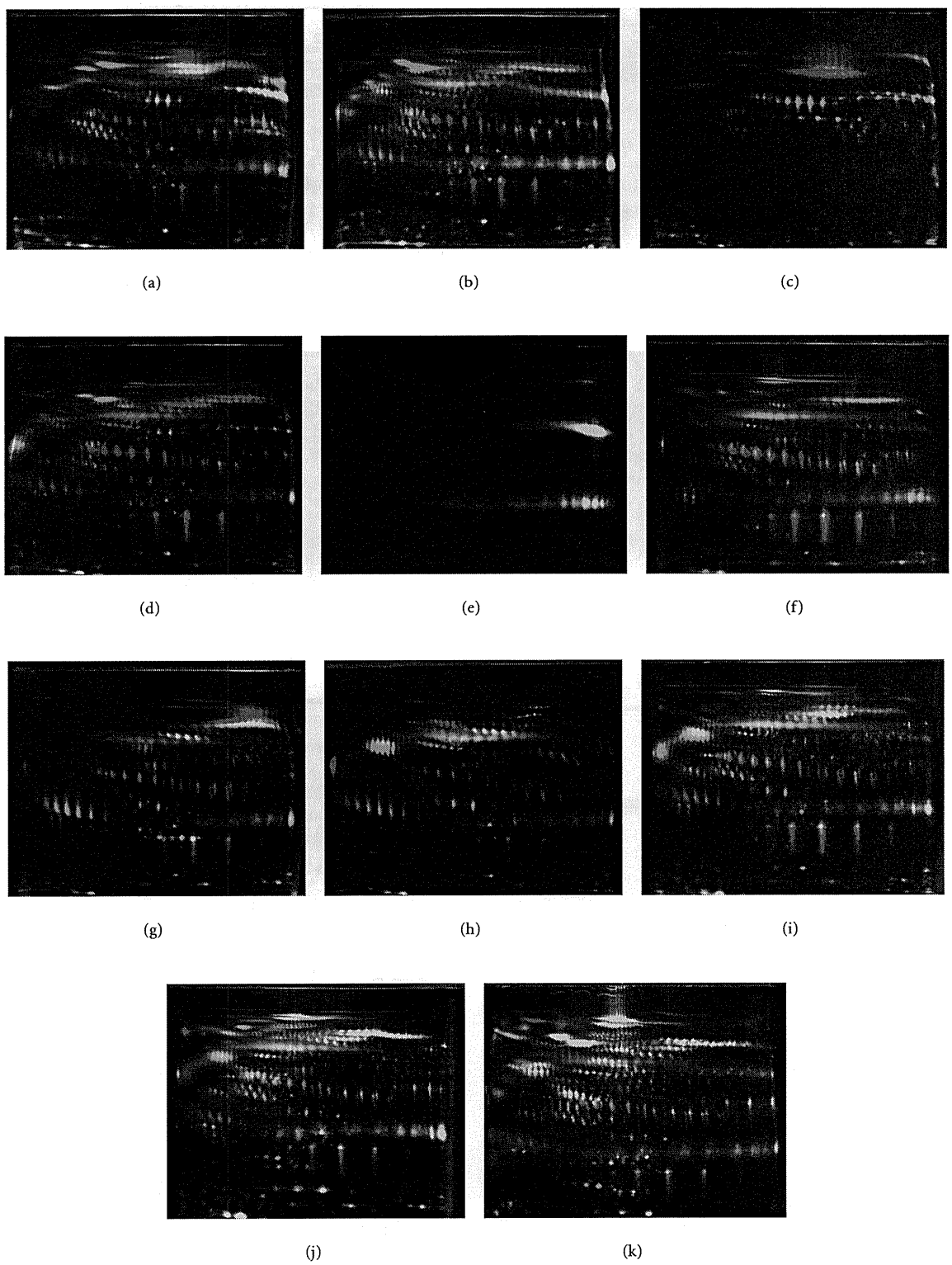

FIGURE 3: Effects of ProteoMiner treatment were examined by 2D-DIGE. The ProteoMiner-treated and untreated samples were labeled with Cy3 and Cy5, respectively, mixed, and separated by 2D gel electrophoresis. Note that a significant number of protein spots showed different intensities between the 2 samples. The dye-swapped images are shown in Supplementary Figure 2. (a) Original plasma; (b) flow-through fraction of HiTrap Blue HP column; (c) binding fraction of HiTrap Blue HP column. (d) Flow-through fraction of HiTrap Protein G HP column. (e) Binding fraction of HiTrap Protein G HP column; 0 mM fraction. (f) 100 mM fraction. (g) 150 mM. (h) 200 mM. (i) 250 mM. (j) 1 M fraction. (k) Resource Q column.

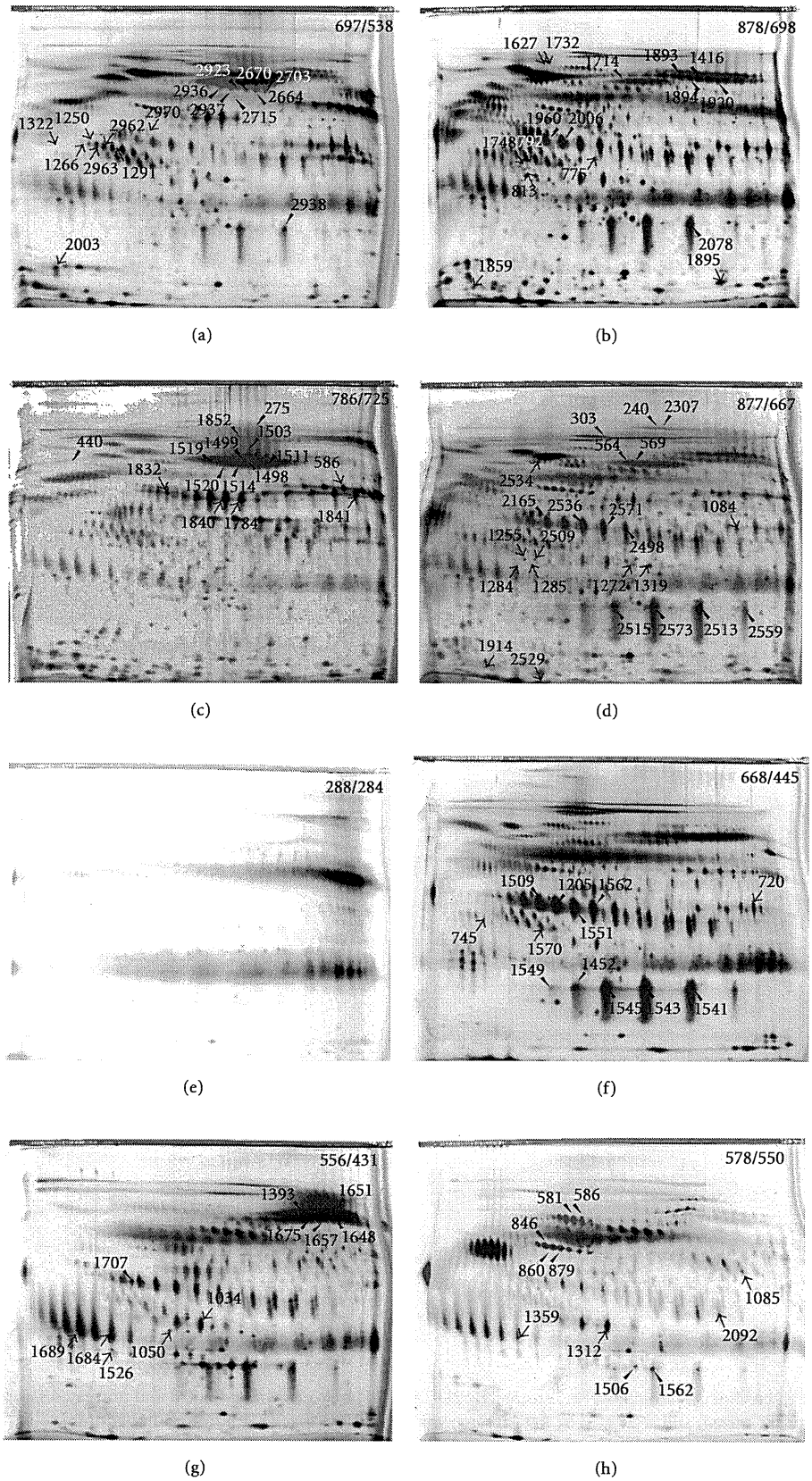

FIGURE 4: Continued.

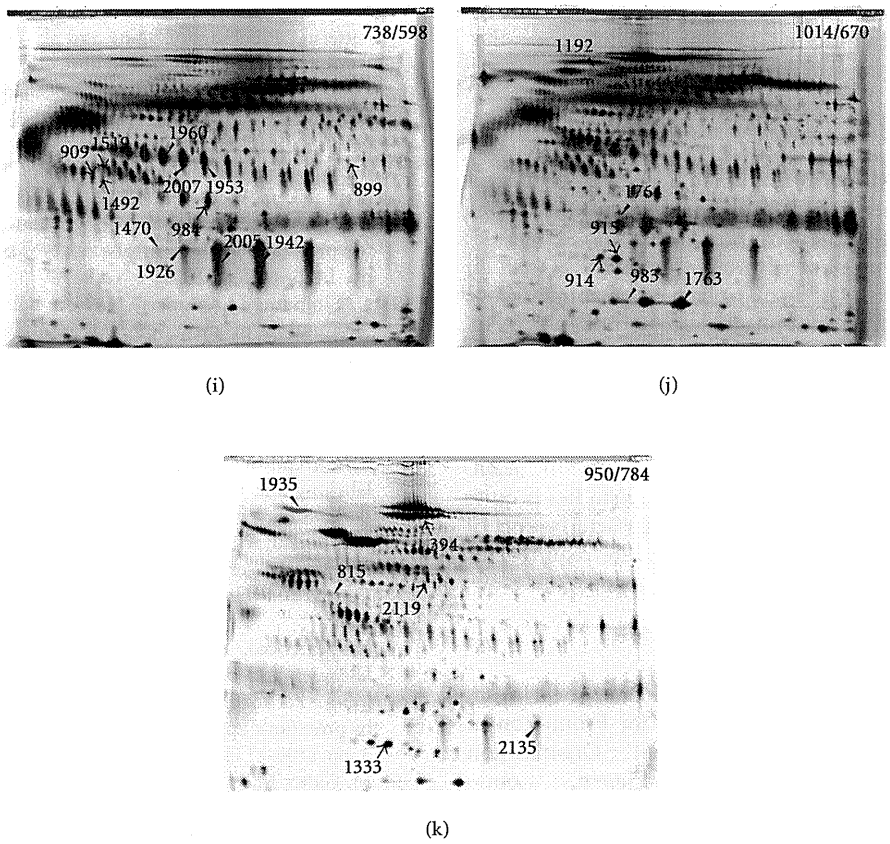

FIGURE 4: Localization of protein spots showing different intensities between the ProteoMinor-treated and untreated samples. Panels (a–k) correspond to those in Figure 3. The protein spot numbers corresponds to those in Supplementary Tables 5 and 6. −/−: number of protein spots without ProteoMiner treatment/those with ProteoMiner treatment.

2D-DIGE increased significantly. This approach may pave a way to a novel strategy for intact plasma proteomics. In contrast, the present results of mass spectrometric protein identification did not support the use of a solid-phase hexapeptide ligand library to enrich low-abundance proteins. It may be because our present approach had 3 limitations. First, mass spectrometric identification was performed for proteins with a greater prominent difference between the samples with or without ProteoMiner treatment, and only 128 of 200 proteins were successfully identified (Supplementary Table 4), probably because of the low protein amount. Proteins with a smaller difference or amount may include trace proteins. Although we optimized the protocols for mass spectrometric protein identification because the sensitivity of the fluorescent dye in the 2D-DIGE was very high, not all protein spots on 2D-DIGE could be identified by mass spectrometry. To evaluate enriched proteins, the complementary use of an LC-MS/MS shotgun approach may be worth considering. Second, proteins from ProteoMiner were recovered by a single-step elution with 8 M urea, 2% CHAPS, and 5% acetic acid, according to the manufacturer's instructions (Bio-Rad). However, because proteins may have interacted with hexapeptide ligand libraries in all possible modes, the absolute elution process may require sequential steps or more stringent buffer conditions such as boiling 10% SDS with 3% DTE [41]. Furthermore, various binding conditions may also be worth considering to capture whole binding proteins [9]. Third, considering the practical use of trace proteins in a biomarker study, we used as much sample as possible for identifying them and examined 10 mL plasma samples as an initial source. However, a larger volume of plasma sample, such as 100 mL, might be needed to collect rare proteins. In practice, such a high volume of plasma is rarely obtained for many cases in biomarker studies, and we may need to optimize the protocols for use of 10 mL plasma. For instance, we identify the biomarker candidates using 100 mL plasma, and using specific antibody against the identified candidate, we will be able to screen a relatively large number of samples with 10 mL volume or less.

The combined use of the ProteoMiner and the proteomic modalities in this study may enable the quantitative comparison for biomarker studies. We demonstrated that the liquid chromatography was quantitatively reproducible (Supplementary Figure 1), and the quantitative reproducibility of the ProteoMiner and 2D-DIGE was previously reported [10, 17]. We may further need to examine how the combined